A generalized upper bound solution for bimetallic rod extrusion through arbitrarily curved dies

H. Haghighat*
Assistant Professor

G.R. Asgari†
Lecturer

In this paper, an upper bound approach is used to analyze the extrusion process of bimetallic rods through arbitrarily curved dies. Based on a spherical velocity field, internal, shearing and frictional power terms are calculated. The developed upper bound solution is used for calculating the extrusion force for two types of die shapes: a conical die as a linear die profile and a streamlined die shape as a curved die profile. The bimetallic rod extrusion process is also simulated by using the finite element code, ABAQUS for those two die shapes. The analytical results have been compared with finite element data and the experimental results obtained from a reference to illustrate the validity of the proposed upper bound solution. These comparisons show a good agreement.

Keyword: Bimetallic rod, Extrusion, Upper bound

1 Introduction

The bimetallic rods consisting of two different material layers have advantages, which are not achievable in a mono-metal rod. The compressive state of stress in extrusion makes this process a suitable choice for producing bimetal rods [1]. In this process, alike other metal forming processes, estimation and minimization of the extrusion force is important. The upper bound technique as an analytical method and the finite element method have been widely used for the analysis of the extrusion of rods made of bimetallic materials. Osakada et al. described the hydrostatic extrusion of composite rods with hard cores through conical dies by the upper bound method [2]. Ahmed studied the extrusion of copper clad aluminum wire [3]. Avitzur summarized the factors, which affect simultaneous flow of layers in extrusion of a bimetal rod through conical dies [4]. Some of these factors include percentage reduction in area, semi-die angle, friction factor between sleeve and die wall, and ratio of core to sleeve radii. Tokuno and Ikeda verified the deformation in extrusion of composite rods by experimental and upper bound methods [5]. Yang et al. studied the axisymmetric extrusion of composite rods through curved dies by experimental and upper bound methods [6]. Sliwa described the plastic zones in the forward extrusion of metal composites by experimental and upper bound methods [7]. Chitkara and Aleem theoretically studied the mechanics of

*Corresponding author, Assistant Professor, Mechanical Engineering Department, Razi University, Kermanshah, hhaghighat@razi.ac.ir
† Lecturer, Payam Higher Education Institute, Golpayegan, ghreza.asgari@gmail.com

extrusion of axisymmetric bimetallic tubes from solid circular billets using fixed mandrel with application of generalized upper bound and slab method analyses [8, 9]. They investigated the effect of different parameters such as extrusion ratio, frictional conditions, and shape of the dies and that of the mandrels on the extrusion pressures. Kang et al. designed the die for hot forward and backward extrusion process of Al-Cu clad composite by experimental investigations and FEM simulations [10]. Hwang et al. studied the plastic deformation behavior within a conical die during composite rod extrusion by experimental and upper bound methods [11]. Kazanowski et al. discussed the influence of initial bi-material billet geometry on the final product dimensions [12]. The flat face die was used for all experiments and the proposed bi-material billet design modifications were evaluated experimentally and by finite element modeling using the Deform 3D system. Nowotynska and Smykla studied the influence of die geometric parameters on plastic flow of layer composites during extrusion process by experimental method [13]. Khosravifard and Ebrahimi [14] analyzed the extrusion of Al/Cu bimetal rod through conical dies by FEM using ANSYS LS-DYNA software and studied the effects of the extrusion parameters in creation of interfacial bonds.

In the past, due to the difficulty in manufacturing of non-conical dies, most research works concerned with the bimetallic rod extrusion, focused on conical dies. Nowadays, by use of computer numerical control machines, manufacturing of curved die shapes is easy and they can be used for bimetal rod extrusion.

The purpose of this paper is to develop an upper bound model for flow of bimetallic rod during extrusion through arbitrarily curved dies. Based on this model, for a given die shape and process parameters, optimum die length and extrusion force are derived. FEM simulation on the extrusion of a bimetallic rod composed of a copper sleeve layer and an aluminum core layer is also conducted.

2 Upper bound analysis

Based on the upper bound theory, for a rigid-plastic Von-Misses material and amongst all the kinematically admissible velocity fields, the actual one that minimizes the power required for material deformation is expressed as [15]

$$J^* = \frac{2}{\sqrt{3}}\sigma_0 \int_V \sqrt{\frac{1}{2}\dot{\varepsilon}_{ij}\dot{\varepsilon}_{ij}}\, dV + \frac{\sigma_0}{\sqrt{3}}\int_{S_v} |\Delta v| dS + m\frac{\sigma_0}{\sqrt{3}}\int_{S_f} |\Delta v| dS - \int_{S_t} T_i v_i dS \tag{1}$$

where σ_0 is the mean flow stress of the material, $\dot{\varepsilon}_{ij}$ the strain rate tensor, m the constant friction factor, V the volume of plastic deformation zone, S_v and S_f the area of velocity discontinuity and frictional surfaces respectively, S_t the area where the tractions may occur, Δv the amount of velocity discontinuity on the frictional and discontinuity surfaces and v_i and T_i are the velocity and tractions applied on S_t, respectively.

Figure (1) is a schematic diagram of the bimetallic rod extrusion through a die of arbitrary curved shape. An initially billet, made up of a rod and an annular tube of two different ductile materials with the mean flow stresses, σ_c and σ_s, respectively, is considered. The subscripts c and s denote core and sleeve, respectively. The initial outer and inner radius of the

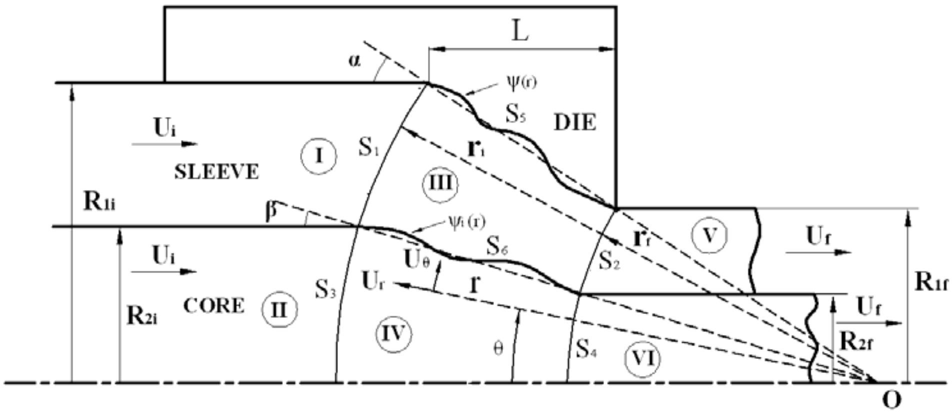

Figure 1 Schematic diagram showing axisymmetric extrusion of a bimetallic rod extrusion

combined billet is R_{1i} and R_{2i}, respectively. The outer radius of the extruded bimetallic rod is R_{1f} and the interface radius of the final extruded rod is R_{2f}.

To analyze the process, the material under deformation is divided into six zones, as shown in figure (1). A spherical coordinate system (r,θ,ϕ) is used to describe the position of the four surfaces of velocity discontinuity as well as the velocity in deformation zones. The position of the coordinate system origin, point O, is defined by the intersection of a line that goes through the point where the die profile starts and the outlet of the die, with axis of symmetry. In zones I and II, the incoming materials are assumed to flow horizontally as rigid body with velocity U_i. In zones V and VI, the extruded materials are assumed to flow horizontally as rigid body with velocity U_f. Zones III and IV are the deformation regions, where the velocity is complex. These zones are surrounded by four velocity discontinuity surfaces S_1, S_2, S_3 and S_4. In addition to these surfaces, there are two frictional surfaces between sleeve surface and core, S_6, and die wall and sleeve, S_5.

The surfaces S_1 and S_3 are located at distance r_i from the origin and the surfaces S_2 and S_4 are located at distance r_f from the origin. The mathematical equations for radial positions of four velocity discontinuity surfaces S_1, S_3 and S_2, S_4 are given by

$$r_i = \frac{R_{1i}}{\sin\alpha} \quad r_f = \frac{R_{1f}}{\sin\alpha} \tag{2}$$

where α is the angle of the line connecting the initial point of the curved die to the final point of the die and

$$\tan\alpha = (R_{1i} - R_{1f})/L \tag{3}$$

where L denotes die length. The die surface, which is labelled as $\psi(r)$ in Figure (1), is given in the spherical coordinate system. For the conical die shape, this function has a single constant value, i.e. $\psi(r) = \alpha$. The interface surface between the inner and the outer materials is defined by $\psi_i(r)$ which is the angular position of the interface surface as a function of the radial distance
from the origin. Angle β, shown in Figure (1), is given by

$$\sin\beta = \frac{R_{2i}}{R_{1i}}\sin\alpha \tag{4}$$

The first step in the upper-bound analysis is to choose an admissible velocity field for the material undergoing plastic deformation. In this study, the velocity field developed by Gordon et al. [16] for mono-metal rod extrusion is extended to bimetallic rod extrusion. The analytical form of the velocity fields in the deformation zones, zones III and IV, are

$$
\begin{gathered}
U_r = -U_f \left(\frac{r_f}{r}\right)^2 \frac{\sin^2\alpha}{\sin^2\psi}\cos\theta \\
U_\theta = -U_f \frac{r_f^2}{r}\frac{\partial\psi}{\partial r}\left(\frac{\sin\alpha}{\sin\psi}\right)^2 \frac{\sin\theta}{\tan\psi} \\
U_\phi = 0
\end{gathered} \tag{5}
$$

where angle ψ is the angular position of a point on the die profile. Based on the mentioned velocity field, the strain rate fields for zones III and IV can be obtained by

$$
\begin{gathered}
\dot{\varepsilon}_{rr} = \frac{\partial U_r}{\partial r} \\
\dot{\varepsilon}_{\theta\theta} = \frac{1}{r}\frac{\partial U_\theta}{\partial\theta} + \frac{U_r}{r} \\
\dot{\varepsilon}_{\phi\phi} = \frac{1}{r\sin\theta}\frac{\partial U_\phi}{\partial\phi} + \frac{U_r}{r} + \frac{U_\theta}{r}\cot\theta \\
\dot{\varepsilon}_{r\theta} = \frac{1}{2}\left(\frac{\partial U_\theta}{\partial r} - \frac{U_\theta}{r} + \frac{1}{r}\frac{\partial U_r}{\partial\theta}\right) \\
\dot{\varepsilon}_{\phi r} = \frac{1}{2}\left(\frac{\partial U_\phi}{\partial r} - \frac{U_\phi}{r} + \frac{1}{r\sin\theta}\frac{\partial U_r}{\partial\phi}\right) \\
\dot{\varepsilon}_{\theta\phi} = \frac{1}{2}\left(\frac{1}{r\sin\theta}\frac{\partial U_\theta}{\partial\phi} + \frac{1}{r}\frac{\partial U_\phi}{\partial\theta} - \frac{\cot\theta}{r}U_\phi\right)
\end{gathered} \tag{6}
$$

With the strain rate field and the velocity field, the standard upper bound method can be implemented. This upper bound method involves calculating the internal power of deformation over the deformation zone volume, calculating the shear power losses over the surfaces of velocity discontinuity (shear surfaces), and the frictional power losses over frictional surfaces.

2-1 Internal power of deformation

The internal power of deformation is given by [15]

$$
\dot{W}_i = \frac{2}{\sqrt{3}}\sigma_0 \int_V \sqrt{\frac{1}{2}\dot{\varepsilon}_{ij}\dot{\varepsilon}_{ij}}\, dV \tag{7}
$$

where σ_0 is the mean flow stress of the material and dV is a differential volume in the deformation zone. Internal power of zones I, II and V, VI are zero and the general equation to calculate the internal power of deformation in zone III that is surrounded by two velocity discontinuity surfaces, S_1 and S_2, interface surface as well as the die surface, is calculated as

$$\dot{W}_{i3} = \frac{4\pi}{\sqrt{3}}\sigma_s \int_{r_f}^{r_i}\int_{\psi_i}^{\psi}\sqrt{\frac{1}{2}\dot{\varepsilon}_{rr}^2 + \frac{1}{2}\dot{\varepsilon}_{\theta\theta}^2 + \frac{1}{2}\dot{\varepsilon}_{\phi\phi}^2 + \dot{\varepsilon}_{r\theta}^2}\ (r\sin\theta) r\, d\theta\, dr \tag{8}$$

where σ_s is the mean flow stress of sleeve and is determined by [8]

$$\sigma_s = \frac{\int_0^{\varepsilon}\sigma\, d\varepsilon}{\varepsilon}, \qquad \varepsilon = \ln\frac{R_{1i}^{\ 2} - R_{2i}^{\ 2}}{R_{1f}^{\ 2} - R_{2f}^{\ 2}} \tag{9}$$

and $\psi_i(r)$ is the angular position of the interface surface as a function of the radial distance from the origin O and it is assumed that

$$\psi_i(r) = \sin^{-1}\left[\frac{\sin\beta}{\sin\alpha}\sin\psi(r)\right] \tag{10}$$

The general equation to calculate the internal power of deformation in zone IV that is surrounded by two velocity discontinuity surfaces, S_3 and S_4, as well as the interface surface, is calculated as

$$\dot{W}_{i4} = 2\pi\frac{2\sigma_C}{\sqrt{3}}\int_{rf}^{r_i}\int_0^{\psi_i}\sqrt{\frac{1}{2}\dot{\varepsilon}_{rr}^2 + \frac{1}{2}\dot{\varepsilon}_{\theta\theta}^2 + \frac{1}{2}\dot{\varepsilon}_{\phi\phi}^2 + \dot{\varepsilon}_{r\theta}^2}\ (r\sin\theta) r\, d\theta\, dr \tag{11}$$

where σ_c is the mean flow stress of core and is given by [8]

$$\sigma_c = \frac{\int_0^{\varepsilon}\sigma\, d\varepsilon}{\varepsilon}, \qquad \varepsilon = \ln\frac{R_{2i}^{\ 2}}{R_{2f}^{\ 2}} \tag{12}$$

2-2 Shear power dissipation

The general equation for the power losses along a shear surface of velocity discontinuity in an upper bound model is [15]

$$\dot{W}_S = \frac{\sigma_0}{\sqrt{3}}\int_{S_v}|\Delta v|\, dS \tag{13}$$

where for velocity discontinuity surfaces S_1 and S_3 [16]

$$\Delta v_{S_1} = U_i \sin\theta + \frac{U_i r_i \left.\frac{\partial\psi}{\partial r}\right|_{r=r_i}\sin\theta}{\tan\alpha} \tag{14}$$

$$dS_1 = 2\pi r_i^2 \sin\theta\, d\theta \tag{15}$$

For velocity discontinuity surfaces S_2 and S_4 [16]

$$\Delta v_{S_2} = U_f \sin\theta + \frac{U_f r_f \left.\frac{\partial\psi}{\partial r}\right|_{r=r_f}\sin^2\theta}{\tan\beta} \tag{16}$$

$$dS_2 = 2\pi r_f^2 \sin\theta\, d\theta \tag{17}$$

Inserting Eqs. (14)-(17) into Eq. (13), the power dissipated on the velocity discontinuity surfaces S_1, S_2, S_3 and S_4 are determined as

$$\dot{W}_{S_1} = 2\pi \frac{\sigma_s r_i^2}{\sqrt{3}} \int_{\beta}^{\alpha} \left| \Delta v_{S_1} \right| \sin\theta \, d\theta \tag{18}$$

$$\dot{W}_{S_2} = 2\pi \frac{\sigma_s r_f^2}{\sqrt{3}} \int_{\beta}^{\alpha} \left| \Delta v_{S_2} \right| \sin\theta \, d\theta \tag{19}$$

$$\dot{W}_{S_3} = 2\pi \frac{\sigma_c r_i^2}{\sqrt{3}} \int_{0}^{\beta} \left| \Delta v_{S_1} \right| \sin\theta \, d\theta \tag{20}$$

$$\dot{W}_{S_4} = 2\pi \frac{\sigma_c r_f^2}{\sqrt{3}} \int_{0}^{\beta} \left| \Delta v_{S_2} \right| \sin\theta \, d\theta \tag{21}$$

2-3 Frictional power dissipation

The general equation for the frictional power losses along a surface with a constant friction factor m is [15]

$$\dot{W}_f = m \frac{\sigma_0}{\sqrt{3}} \int_{S_f} \left| \Delta v \right| dS \tag{22}$$

For frictional surface S_5:

$$\left| \Delta v_5 \right| = \left| U_r \cos\eta + U_\theta \sin\eta \right|_{\theta=\psi} \tag{23}$$

where η is the local angle of the die surface with respect to the local radial velocity component and it can be determine as [16]

$$\cos\eta = \frac{1}{\sqrt{1+(r\dfrac{\partial\psi}{\partial r})^2}}, \quad \sin\eta = \frac{r\dfrac{\partial\psi}{\partial r}}{\sqrt{1+(r\dfrac{\partial\psi}{\partial r})^2}} \tag{24}$$

and

$$dS_5 = 2\pi r \sin\psi \sqrt{1+(r\frac{\partial\psi}{\partial r})^2} \, dr \tag{25}$$

Replacing Eqs. (23)-(25) into Eq. (22), the power dissipated on the die surface can be determined as

$$\dot{W}_{f5} = 2\pi \frac{m_1 \sigma_s}{\sqrt{3}} \int_{r_f}^{r_i} \left| \Delta v_5 \right| r \sin\psi \, d\psi \tag{26}$$

Where m_1 is the constant friction factor between sleeve and die.

Based on the model, the total power needed for a bimetallic rod extrusion process can be obtained by summing the internal power and the power dissipated on all frictional and velocity discontinuity surfaces. Then

$$\dot{W} = \dot{W}_{i3} + \dot{W}_{i4} + \dot{W}_{s1} + \dot{W}_{s2} + \dot{W}_{s3} + \dot{W}_{s4} + \dot{W}_{f5} \tag{27}$$

Therefore, the total upper bound solution for extrusion force is given by

$$F = \frac{J^*}{U_i} \tag{28}$$

A MATLAB program has been implemented for the previously derived equations and was used to study the plastic deformation for different die shapes and friction conditions. It includes a parameter L, die length, that should be optimized.

3 Results and discussion

To make a comparison with the developed model, a bimetal rod composed of aluminum as core layer and copper as sleeve layer, was used. The configuration of the sleeve and core layers is shown in figure (2). The flow stresses for copper and aluminum were obtained as [11]

$$\begin{aligned} \sigma_{Al} &= 189.2\ \varepsilon^{0.239}\ \text{MPa} \\ \sigma_{cu} &= 335.2\ \varepsilon^{0.113}\ \text{MPa} \end{aligned} \tag{29}$$

Friction factors $m_1 = 0.2$ and $m_2 = 0.9$ [11] were adopted during the analytical solution and the FEM simulation.

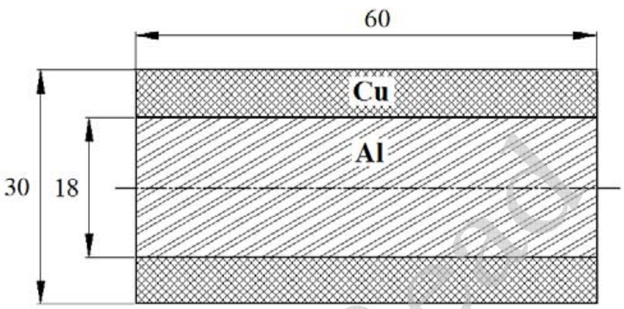

Figure 2 Configuration of the bimetallic rod before extrusion (dimensions are in mm)

The developed upper bound model can be use for bimetallic rod extrusion through dies of any shape if the die profile is expressed as equation $\psi(r)$. Two types of die shapes are examined in the present investigation. The first die shape is conical die. This profile has a single constant value, i.e. $\psi(r) = \alpha$. The second die shape is from the work by Yang and Han [17]. They created a streamlined die shape as a fourth-order polynomial whose slope is parallel to the axis at both entrance and exit. Die shape of Yang and Han was expressed in spherical coordinate system by Ref. [18].

The extrusion process is simulated by using the finite element code, ABAQUS. Considering the symmetry in geometry, two-dimensional axisymmetric models are used for FEM analyses. In each case, the whole model is meshed with CAX4R elements. Punch and die undergo elastic strain only. Thus, it is not necessary to use a fine mesh in these two pieces. However, sufficiently fine meshing is essential in core and sleeve materials, which undergo plastic deformation. The die model is fixed by applying displacement constraint on its nodes while the punch model is loaded by specifying displacement in the axial direction. Figure 3a illustrates the mesh used to analyze the deformation in extrusion of bimetallic rod with the configuration shown in Figure (2) for Yang and Han die shape. Deformed models of sleeve and core are shown in Figure (3b). This figure shows that the aluminum leaves the deformation zone sooner than the copper. Since flow stress of aluminum is lower than copper, the former extrudes first. As the applied stress increases to flow stress of copper, simultaneous flow of the two metals continues.

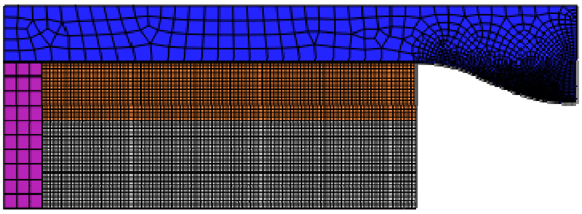

(a) The finite element mesh

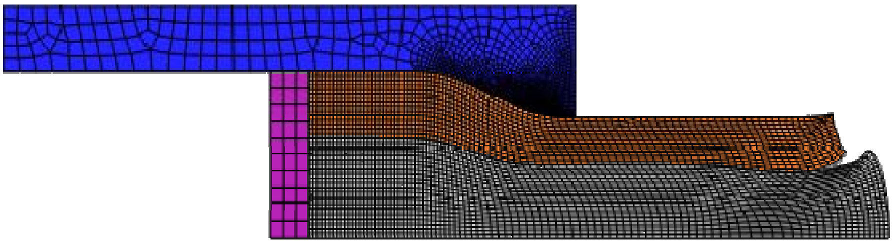

(b) The deformed mesh

Figure 3 (a) The finite element mesh and (b) the deformed mesh, in bimetallic tube extrusion

In figure (4), the extrusion forces obtained from the upper bound solution are compared with the experimental results obtained from Ref. [11] for conical die with $\alpha = 15^{\circ}$ and three different reductions in areas, RA=25, 50 and 66.7%. The results show good agreement between the analysis and experiment.

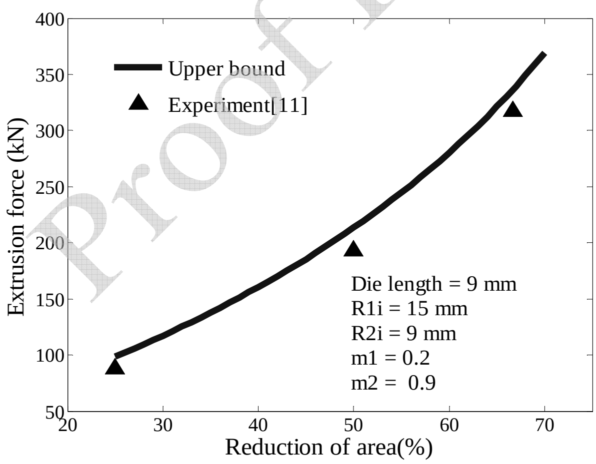

Figure 4 Comparison of analytical, FEM and experimental data [11] for conical die

In figure (5), the extrusion forces obtained by upper bound and FEM solutions for the Yang and Han die shape are compared. The results show a good agreement between the upper bound data and the FEM results. It is observed that, there is an optimal die length, which minimizes the extrusion force.

In figure (6), extrusion force of conical die and the Yang and Han die shape obtained from the upper bound approach are compared with each other. The extrusion force of Yang and Han die shape is lower than conical die. Because this curved die has a smooth transition at the die entrance and exit and shearing in the velocity discontinuity surfaces is zero.

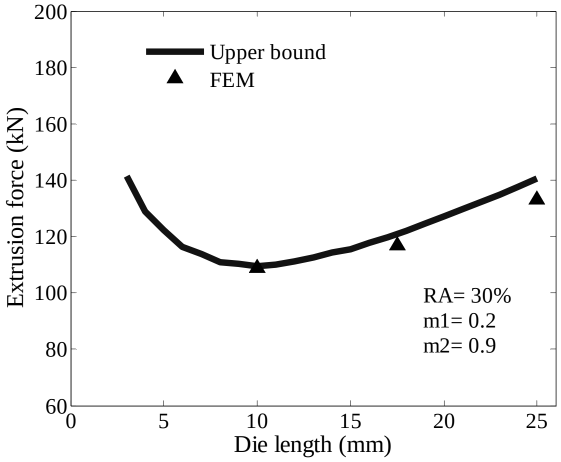

Figure 5 Comparison of analytical and FEM results for Yang and Han die shape

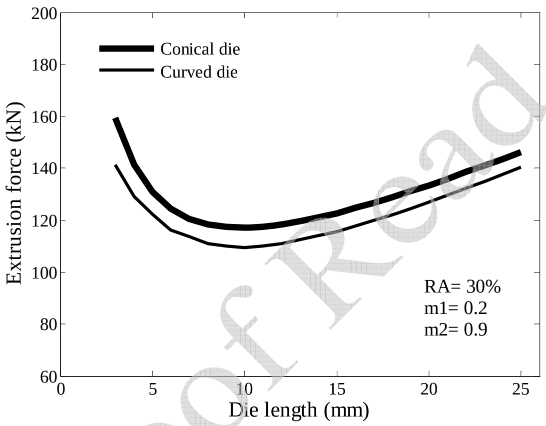

Figure 6 Comparison between the theoretical extrusion force values versus die length for conical and curved dies

The effect of die length on the extrusion force for different values of friction factor is shown in Figure (7). As it is expected, for a given value of friction factor, the extrusion force is minimized in an optimum die length. It is observed that the optimum die length decreases when shearing

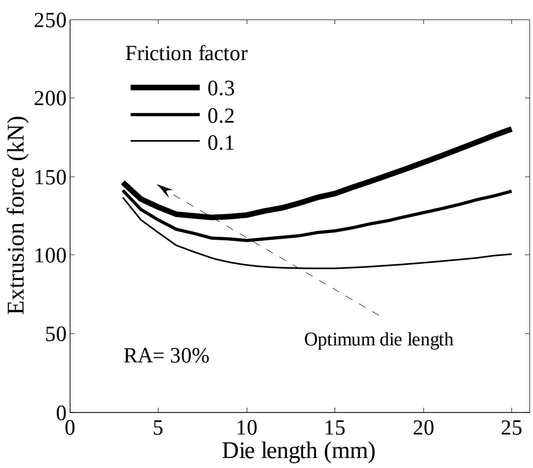

Figure 7 The effect of die length on the extrusion force for different values of friction factor

friction factor increases. This figure, also, shows that an increase in the friction factor tends to increase the extrusion force.

Since the developed upper bound solution is faster than FEM analysis, it can be very beneficial in studying the influence of multiple variables on the bimetallic rod extrusion process and for a given die shape, it can be used for finding the optimum die length which minimizes the extrusion force.

4 Conclusions

In this research, a published velocity field for mono-metal rod extrusion was extended to bimetallic rod extrusion process. The internal powers and the powers terms, supplied on frictional and shear surfaces, were determined and they were used in upper bound model of bimetallic rod extrusion process through dies of any shape. The results showed a good agreement between the analytical solution, FEM simulation and experiment. The results also showed that the extrusion force of Yang and Han die shape is lower than conical die and the optimum die length decreases when shearing friction factor increases.

The developed upper bound solution can be used for fast estimation of extrusion force of bimetallic rods through dies of any shape and for a given die shape and process parameters, it can be used for finding the optimum die length which minimizes the extrusion force.

References

[1] Berski, S., Dyja, H., Banaszek, G., and Janik, M., "Theoretical Analysis of Bimetal Rod Extrusion Process in Double Reduction Dies", J. Mater Process Technol. Vol. 154, pp. 153–583, (2004).

[2] Osakada, K., Limb, M., and Mellor, P.B., "Hydrostatic Extrusion of Composite Rods with Hard Cores", Int. J. Mech. Sci. Vol. 15, 291-307, (1973).

[3] Ahmed, N., "Extrusion of Copper Clad Aluminum Wire", J. Mech. Work Technol. Vol. 2, pp. 19–32, (1978).

[4] Avitzur, B., "*Handbook of Metal-Forming Processes*", New York, Wiley, (1983).

[5] Tokuno, H., and Ikeda, K., "Analysis of Deformation in Extrusion of Composite Rods", J. Mater Process Technol. Vol. 26, pp. 323-335, (1991).

[6]Yang, D.Y., Kim, Y.G., and Lee, C.M., "An Upper-bound Solution for Axisymetric Extrusion of Composite Rods through Curved Dies", Int. J. Mech. Sci. Vol. 31, pp. 565-575, (1991).

[7] Sliwa, R., "Plastic Zones in the Extrusion of Metal Composites", J. Mater Process Technol. Vol. 67, pp. 29-35, (1997).

[8] Chitkara, N.R., and Aleem, A., "Extrusion of Axi-symmetric Bimetallic Tubes from Solid Circular Billets: Application of a Generalized upper Bound Analysis and some Experiments", Int. J. Mech. Sci. Vol. 43, pp. 2833-2856, (2001).

[9] Chitkara, N.R., and Aleem, A., "Extrusion of Axi-symmetric Bimetallic Tubes: some Experiments using Hollow Billets and the Application of a Generalized Slab Method of Analysis", Int. J. Mech. Sci. Vol. 43, pp. 2857–2882, (2001).

[10] Kang, C.G., Jung, Y.J., and Kwon, H.C., "Finite Element Simulation of Die Design for Hot Extrusion Process of Al/Cu Clad Composite and its Experimental Investigation", J. Mater Process Technol. Vol. 124, pp. 49-56, (2002).

[11] Hwang, Y.M., and Hwang T.F., "An Investigation into the Plastic Deformation Behavior Within a Conical Die during Composite Rod Extrusion", J. Mater Process Technol. Vol. 121, pp. 226-233, (2002).

[12] Kazanowski, P., Epler, M.E., and Misiolek, W.Z., "Bi-metal Rod Extrusion-process and Product Optimization", Mater Sci. and Eng. Vol. 369, pp. 170–180, (2004).

[13] Nowotynska, I., and Smykla, A., "Influence of Die Geometric Parameters on Plastic Flow of Layer Composites during Extrusion Process", J. Mater Process Technol. Vol. 209, pp. 1943-1949, (2009).

[14] Khosravifard, A., and Ebrahimi, R., "Investigation of Parameters Affecting Interface Strength in Al/Cu Clad Bimetal Rod Extrusion Process", Materials and Design, Vol. 31, pp. 493-499, (2010).

[15] Prager, W., and Hodge, P.G., "*Theory of Perfectly Plastic Solids*", John Wiley and Sons Inc., New York, (1951).

[16] Gordon, W.A., Van Tyne, C.J., and Moon, Y.H., "Axisymmetric Extrusion through Adaptable Dies-Part 1: Flexible Velocity Fields and Power Terms", Int. J. Mech. Sci. 2007, Vol. 49, pp. 86–95, (2007).

[17] Yang, D.Y., and Han, C.H., "A New Formulation of Generalized Velocity Field for Axisymmetric Forward Extrusion through Arbitrarily Curved Dies", Transactions of the ASME, J. Eng. Ind. Vol. 109, pp. 161–168, (1987).

[18] Gordon, W.A., Van Tyne, C.J., and Moon, Y.H., "Axisymmetric Extrusion through Adaptable Dies-Part 3: Minimum Pressure Streamlined Die Shapes", Int. J. Mech. Sci. Vol. 49, pp. 104-115, (2007).

Nomenclature

m_1 : friction factor between sleeve and die
m_2 : friction factor between core and sleeve
r, θ, ϕ : spherical coordinates
r_f : spherical radius of exit velocity discontinuity surface
r_i : spherical radius of entrance velocity discontinuity surface
R_{1f} : outer radius of sleeve at exit

R_{2f} : outer radius of core, in extruded bimetallic rod
R_{1i} : radius of container
R_{2i} : outer radius of core in initial bimetallic rod
Δv : amount of velocity discontinuity
L : length of die
S : area of frictional or velocity discontinuity surface
U_r, U_θ, U_ϕ : velocity components in spherical coordinate
U_f : exit velocity
U_i : entrance velocity
J^* : externally supplied power of deformation
$\dot{W}_f$: power dissipated on the frictional surfaces
$\dot{W}_i$: internal power of deformation
$\dot{W}_S$: power dissipated on the velocity discontinuity surfaces

Greek symbols

$\dot{\varepsilon}_{rr}, \dot{\varepsilon}_{\theta\theta}, \dot{\varepsilon}_{\phi\phi}$: normal strain rate components
$\dot{\varepsilon}_{r\theta}, \dot{\varepsilon}_{r\phi}, \dot{\varepsilon}_{\theta\phi}$: shear strain rate components
η : local angle of the die surface with respect to the local radial velocity component
α : angle of the line connecting the initial point of the die to the final point of the die
β : angle of interface surface in deformation zone
$\psi(r)$: angular position of the die as a function of radial position
$\psi_i(r)$: angular position of the interface as a function of radial position
σ_c : mean flow stress of the core material
σ_s : mean flow stress of the sleeve material

چکیده

در این مقاله، فرآیند اکستروژن مستقیم میله های دو فلزی با قالب منحنی به روش کرانه فوقانی تحلیل و به روش اجزا محدود شبیه سازی شده است. با ارایه یک میدان سرعت در دستگاه مختصات کروی، مقادیر توان های داخلی ، توان های برشی و توان های اصطکاکی به دست آمده اند. از حل کرانه بالایی ارایه شده، برای محاسبه نیروی اکستروژن در دو شکل قالب مخروطی و منحنی استفاده شده است. فرآیند اکستروژن دو فلزی در این دو شکل قالب با نرم افزار المان محدود ABAQUS شبیه سازی شده اند. برای اعتبار دهی تحلیل انجام شده، نتایج روش کرانه فوقانی با نتایج به دست آمده از آزمایشهای سایر محققان و شبیه سازی به روش اجزا محدود مقایسه شده اند. این مقایسه تطابق مناسبی را نشان دادند.